OPEN

Experimental Observation of Negative Effective Gravity in Water Waves

Xinhua Hu[1], Jiong Yang[1,2], Jian Zi[2], C. T. Chan[3] & Kai-Ming Ho[4]

[1]Department of Materials Science, Key Laboratory of Micro- and Nano-Photonic Structures (Ministry of Education) and Laboratory of Advanced Materials, Fudan University, Shanghai 200433, China, [2]Department of Physics and Key Laboratory of Surface Physics, Fudan University, Shanghai 200433, China, [3]Department of Physics, Hong Kong University of Science and Technology, Clear Water Bay, Kowloon, Hong Kong, China, [4]Ames Laboratory and Department of Physics and Astronomy, Iowa State University, Ames, Iowa 50011, USA.

The gravity of Earth is responsible for the formation of water waves and usually difficult to change. Although negative effective gravity was recently predicted theoretically in water waves, it has not yet been observed in experiments and remains a mathematical curiosity which is difficult to understand. Here we experimentally demonstrate that close to the resonant frequency of purposely-designed resonating units, negative effective gravity can occur for water waves passing through an array of resonators composing of bottom-mounted split tubes, resulting in the prohibition of water wave propagation. It is found that when negative gravity occurs, the averaged displacement of water surface in a unit cell of the array has a phase difference of π to that along the boundary of the unit cell, consistent with theoretical predictions. Our results provide a mechanism to block water waves and may find applications in wave energy conversion and coastal protection.

G ravitation, or gravity, is a natural phenomenon that a body attracts another one with a force proportional to their masses. Due to the gravity of Earth, a body on Earth can possess weight and fall to the ground with an increasing speed when dropped. If air resistance is neglected, the corresponding acceleration g_0 is the same for all objects no matter what are their compositions and masses[1]. This effect was first discovered by Galileo Galilei in the late 16th century and becomes the starting point of modern physics.

Gravitation is also responsible for complex phenomena including the motions of celestial bodies and the formation of water waves in seas. Under the restoring force provided by gravity, water waves propagate on the surface of water and their velocities depend on both the gravitational acceleration g_0 and water depth[2]. Such mechanical waves can interact with a host of periodic structures such as rippled bottoms[3–10], floating disk arrays[11] and vertical cylinder arrays[12–17]. Recently, inspired by the research of metamaterials[18–34], a concept of effective liquid was proposed to describe the interaction of water waves with periodic structures[35,36]. This concept states that for wavelengths much longer than the period, the water with a periodic structure can be viewed as a homogeneous liquid characterized by an effective depth h_e and effective gravitational acceleration g_e[35,36]. Interestingly, it was theoretically found that the effective gravity can be different from the one on the Earth ($g_e \neq g_0$) in some cases[35,36]. For example, an increased gravity ($g_e > g_0$) is found in water pierced by a cylinder array[35], resulting in a new type of water wave refraction[15,16]. For water with a resonator array, the effective gravity can even be negative ($g_e < 0$) near resonant frequency, so that water waves cannot propagate through the resonator array[36]. These results promise a new mechanism to control the propagation of water waves, which have applications in wave energy conversion and coastal protection[37–41]. However, the exotic effects, especially the negative gravity, have not yet been observed in experiments and remain mathematical curiosities which are difficult to understand.

Here we report on experimental observation of the negative effective gravity for water waves through an array of resonators of bottom-mounted split tubes. A displacement averaging method is proposed to obtain and understand the effective gravity. Based on simulations and measurements, it is found that when negative gravity occurs, the averaged displacement of water surface in a unit cell of the array has a phase difference of π to that along the boundary of the unit cell. In contrast, the phase difference is zero for positive gravity.

Results

Sample constructions and the effective medium theory. The system under study is a channel of water pierced by a periodic array of vertical bottom-mounted split tubes (Figs. 1a and 1b). The width of the channel w equals to the periodicity a of 12 mm. The water depth h_0 is 8 mm. Each split tube has an outer radius r_1 of 4 mm, inner radius r_2 of 3 mm and slit width Δ of 1 mm and supports a resonant mode for water waves. Here, water waves outside the
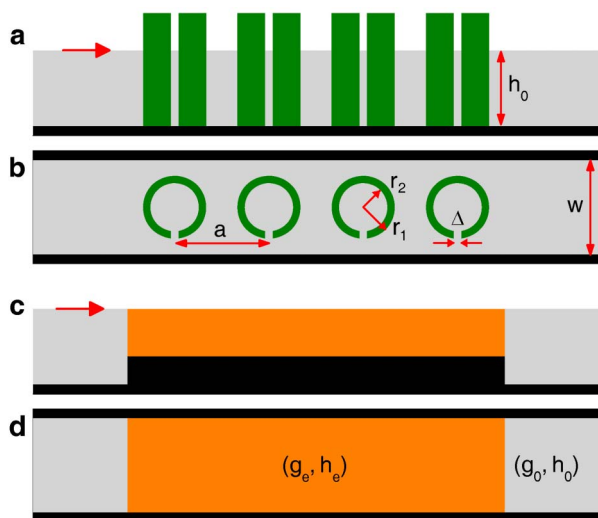
Figure 1 | Water waves propagating through a resonator array and the corresponding effective medium description. (a) Side view and (b) top view of four resonators of vertical bottom-mounted split tubes placed in a channel of water. The split tubes are made of copper and have outer radius $r_1 = 4$ mm, inner radius $r_2 = 3$ mm, slit width $\Delta = 1$ mm, height of 15 mm and spacing $a = 12$ mm. The water depth $h_0 = 8$ mm and channel width $w = 12$ mm. (c) Side view and (d) top view of a homogeneous liquid (orange part) with an effective gravitational acceleration g_e and effective depth h_e. For water waves with long wavelengths, the water with a resonator array shown in Fig. 1a can be replaced by the effective liquid shown in Fig. 1c.

Figure 2 | Observation of the negative effective gravity in water waves. (a) Effective reduced depth u_e, (b) effective gravitational acceleration g_e and (c) transmission as a function of frequency for water with a resonator array as shown in Fig. 1. The solid lines, dashed curves and red squares are obtained from effective medium theory, simulations and experiments, respectively. Due to negative gravity (yellow part in Fig. 2b), a transmission dip is observed at 4.4 Hz in Fig. 2c. (d–e) The same as (a–c) but for four bottom-mounted cylinders with radius of 4 mm.

tube cause the water in the slit to oscillate in and out, resulting in the vibration of the water surface in the tube[36]. Such a Helmholtz mode has a resonant wavenumber $k_r \approx \sqrt{\Delta/(\pi r_2^2 d)}$ and loss γ_k, where $d \approx r_1 - r_2 + 0.6\Delta$ is the effective neck length of the Helmholtz resonator [see Supplementary information for details]. From the wavenumber k, the angular frequency of water waves can further be obtained by the dispersion of $\omega = \sqrt{guk}$, where the reduced water depth $u = \tanh(kh)/k$ with h being the water depth. We note that the dispersion is valid for both water and effective liquid, when subscripts 0 and e are added under the variables of g, h, u and k, respectively.

For water with a split tube array, the corresponding effective liquid (Figs. 1c and 1d) possesses an effective gravitational acceleration[36]

$$g_e = g_0 / \left[1 + \frac{f_s k_0^2}{k_r^2 - k_0(k_0 + i\gamma_k)}\right] \quad (1)$$

and effective reduced depth of $u_e = u_0(1 - f_s)/(1 + f_s)$, where the filling ratio of split tubes $f_s = \pi r_1^2/a^2$. Hence, our sample has a positive effective reduced depth ($u_e = 0.48u_0$, Fig. 2a) and frequency-dependent effective gravitational acceleration (Fig. 2b). For frequencies ranging from 4.1 Hz to 4.85 Hz (called resonant gap), the effective gravity becomes negative ($g_e < 0$) so that surface waves cannot propagate through the split tube array.

Verification of the negative effective gravity from transmission measurements. To experimentally verify the existence of negative gravity, we measured the transmission spectrum for impinging of water waves on the split tube array (Methods), as shown the squares in Fig. 2c. Due to the negative gravity, a transmission dip was observed at 4.4 Hz. The experimental results agree well with the calculated ones based on the effective parameters (solid line in Fig. 2c). We note that the measured transmission data are lower than the theoretical values in the passing bands (with frequencies lower than 4 Hz or between 5 Hz and 6 Hz) because of the
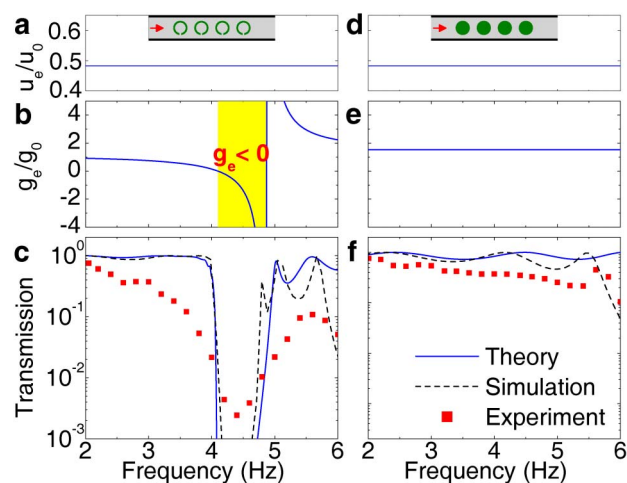
propagation loss, imperfect reflection and surface tension effect at tube walls. Although the surface tension influences slightly the dispersion of water waves here (Methods), it has effects on the water surface near the walls and may increase the propagation loss.

For comparison, a control experiment was also carried out with a control sample where the split tubes were replaced by rigid cylinders of the same outer radius. According to our previous theory[35], water with the cylinder array has the same effective depth (Fig. 2d), but different effective gravitational acceleration ($g_e = g_0/(1 - f_s)$, Fig. 2e), compared with the parameters for a split tube array. Hence, water waves with long wavelengths can propagate through the cylinder array and the above transmission dip induced by negative gravity is not observed here (Fig. 2f). This control experiment confirmed that the negative gravity is induced by local resonance rather than the lattice periodicity.

A new displacement averaging method to obtain the effective gravity. Although the effect of negative gravity has been verified by the transmission experiments, it remains mysterious since it cannot be understood by simple averaging of gravity over area. Here, borrowing the idea from electromagnetic metamaterials, we derive a new displacement averaging formula to obtain and understand the effective gravitational acceleration (see Supplementary information for derivations):

$$g_e = g_0 \langle\eta\rangle_b / \langle\eta\rangle_a \quad (2)$$

Here, $\langle\eta\rangle_b$ is the averaged vertical displacement of water surface along the boundary of a unit cell, representing the boundary excitation. $\langle\eta\rangle_a$ is the averaged displacement over the area of the unit cell, namely the averaged response. The averaged displacements can be further expressed as $\langle\eta\rangle_a = f_s\eta_1 + (1 - f_s)\eta_2$ and $\langle\eta\rangle_b \approx \eta_2$ with η_1 and η_2 being the averaged displacements inside and outside the split tube, respectively. Using a simple hydrodynamics model, it can be proved (see Supplementary information for derivations) that

$$\eta_1 = \eta_2 / \left[1 - k_0(k_0 + i\gamma_k)/k_r^2\right] \quad (3)$$
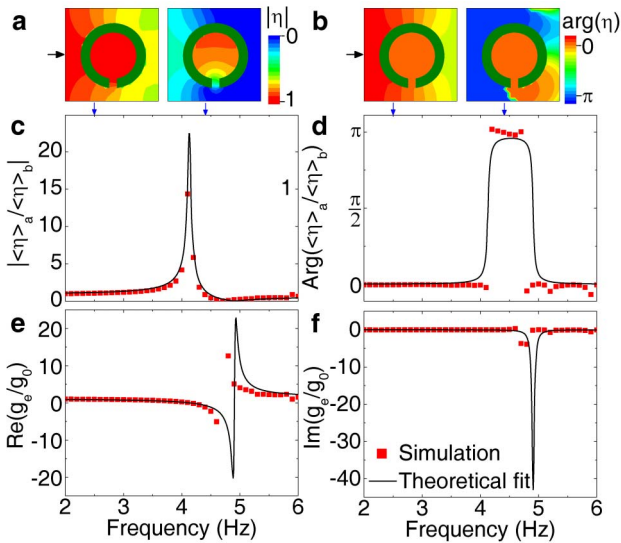
Thus, Eq. (1) can be alternatively derived.

Figure 3 | Understanding of the negative effective gravity by simulated mode profiles. (a) Amplitude and (b) phase profiles of the vertical displacement of water surface η in the leftmost unit cell in Fig. 1b. The left and right panels are for 2.5 Hz (positive gravity) and 4.4 Hz (negative gravity), respectively. (c) Amplitude and (d) phase of η_a/η_b as a function of frequency. η_a and η_b are the averaged η over the area and along the boundary of the unit cell, respectively. The red squares are simulation results and the black curves are theoretical fits. (e) Real and (f) imaginary parts of g_e/g_0 deduced from the results in Figs. 3c and 3d.

Understanding the negative effective gravity by water-wave simulations. From Eq. (2), we can see that for positive gravity, the averaged response in a unit cell has the same phase with the boundary excitation. However, the phase difference becomes π when negative gravity occurs. To confirm the picture of negative gravity, we performed numerical simulations (Methods) for above water wave experiments. The calculated transmission spectra (dashed lines in Figs. 2c and 2f) agree well with experiments and theory, showing the correctness of simulations. Meanwhile, the profiles of displacement of water surface and ratios of response to excitation ($\langle\eta\rangle_a/\langle\eta\rangle_b$) were obtained for different frequencies (Figs. 3a–3d). It can be seen that for a given excitation, the amplitude of response reaches a maximum at resonant frequency (Fig. 3c). In a frequency range above the resonant frequency, the response has a phase difference of π compared with the excitation (Fig. 3d), resulting in a negative gravity (Fig. 3e). By fitting the simulated data of $\langle\eta\rangle_a/\langle\eta\rangle_b$ by the above model, a radiation loss of $\gamma_k = 0.017k_r$ is obtained for the split tube resonators. Due to such intrinsic loss, an imaginary part is also found in the effective gravity (Fig. 3f).

Understanding the negative effective gravity by displacement measurements. In corroboration of the simulations, we measured experimentally the surface displacements for two points inside and outside a split tube (Methods). The surface displacement inside tube η_1 is found to have the highest amplitude, about 7 time of the value η_2 outside tube, at the center frequency of resonant gap (Fig. 4a). Below the resonant frequency of about 4.1 Hz, the surface displacement inside tube has almost the same phase with that outside tube (Fig. 4b). However, above the resonant frequency, the displacements inside and outside tube have different phases and the phase difference increases to π above 5 Hz. The experimental data can be fitted by Eq. (3), showing a higher loss ($\gamma_k = 0.15k_r$) than the ideal case. Due to this loss, the effective gravitational acceleration is not too negative in the real part (Fig. 4c) and has simultaneously an imaginary part (Fig. 4d). As a result, a small amount of transmission (0.2%) has been measured at the dip frequency in Fig. 2c.
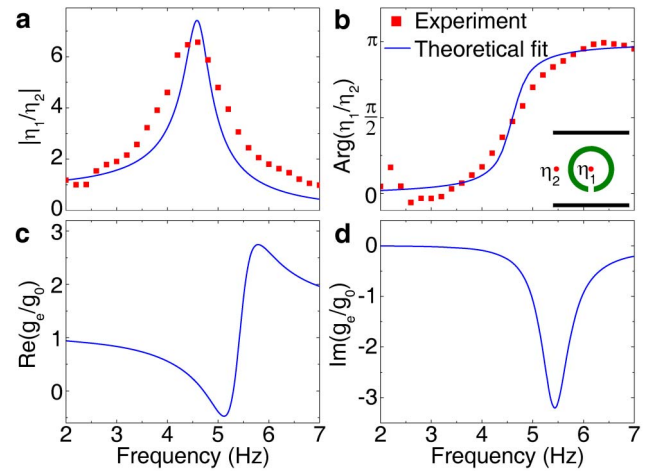

Figure 4 | Understanding of the negative effective gravity by measured surface displacements. (a) Amplitude and (b) phase of η_1/η_2 as a function of frequency. η_1 and η_2 are the vertical displacements of water surface for the two points as shown in the inset of Fig. 4b. The red squares are experimental data and the blue curves are theoretical fits. (c) Real and (d) imaginary parts of g_e/g_0 deduced from the results in Figs. 4a and 4b.

Discussion

By now the negative effective gravity has been observed experimentally and understood by a displacement averaging method. This method can also be applied to understand the increased effective gravity[35] for water with a cylinder array. For a unit cell with a cylinder, the averaged response ($\langle\eta\rangle_a = (1-f_s)\eta_2$) is smaller than the boundary excitation ($\langle\eta\rangle_b \approx \eta_2$ with η_2 being the averaged displacement outside cylinder) so that the increased gravity ($g_e = g_0/(1-f_s)$) can be alternatively obtained.

Due to the negative effective gravity, a low-frequency resonant gap is formed in water waves. Similar resonant gaps also exist for sound waves in metamaterials composed of acoustic Helmholtz resonators, which is interpreted by a negative effective modulus. In the gap with negative modulus, an interesting negative group velocity was found for sounds: for a sound pulse incident on a thin slab of the metamaterial, the peak of transmitted pulse has been detected before the peak of incident pulse enters into the slab[29]. We note that such a "superluminal" phenomenon[32,42] may also been observed in our water-wave system if a wave source of pulse is applied in the water-wave experiment.

Although the negative effective gravity is observed in water with split tubes, it could be achieved by other kinds of resonators. Various resonators such as heaving buoys and underwater pendulums[37–40], have been invented and applied to extract ocean wave energy[38] and resonator arrays have been regarded as a key part of future wave power plants[41]. Our work indicates that when those resonators are arranged in an array, negative gravity or negative depth could be achieved, giving rise to low-frequency stopping bands of water waves. As a result, long wavelength water waves, even including tsunamis, may be blocked by a narrow array of resonators. In addition, if negative gravity and depth are achieved simultaneously, water waves can propagate in a slow and negative velocity through resonator arrays, which may enhance the efficiency of wave energy extraction.

Methods

Experimental set-up. Water is contained in a vessel that is made of Aluminum in four sides and of transparent glass in the bottom. The vessel has a length of 1.4 m and inner width of 12 mm, two vertical long sides and two slanted short sides (where the slopes have a length of 170 mm and height of 10 mm, which can eliminate the reflection of water waves). The vessel is placed horizontally so that the water depth is

constant in the middle part of the vessel. The split tubes are made of copper and placed vertically and firmly in the middle of the vessel.

An air tube with oscillating pressure was used to generate harmonic water surface waves with frequency ranging from 2 Hz to 10 Hz. To generate ideal gravity surface waves in this frequency range, a liquid (CFC-113) with low viscosity and low surface tension was applied to replace water. We note that the wave source and liquid have been adopted in our previous experiments[7,14,17].

A number of parallel light beams (with diameter of ~1 mm) were applied to measure simultaneously the vertical vibration of a few points on the water surface. Here, the light beams went vertically downward, then passed through the water surface and glass bottom and finally projected to a screen under the vessel. When surface waves are generated in the water, the light spots on the screen can oscillate and the oscillations linearly depend on the vibrations of certain points on the water surface.

A digital camera (Panasonic DMC-FX100) was used record the oscillations of light spots on the screen (with 30 frames/second, 600×480 pixels/frame and 20 second for each frequency; see Supplementary Movies S1 and S2). Using the software QuickTime, each recorded movie can be converted into a series of pictures with bmp format. The positions of light spots are then obtained for each picture by using a MATLAB program. Here, the center of a light spot is calculated by a light-intensity-weighted average method so that the accuracy of light spot center can be smaller than 1/200 of a pixel in the digital picture. At last, a Fortran program is used to do Fourier transform for the oscillations of light spots. Using this method, we can obtain at the same time the amplitudes and phases for many points on the water surface, such as the results shown in Figs. 4a and 4b.

Assume only plane waves are generated in the channel of water, namely $\eta(x,t) = \left(Ae^{ik_0x} + Be^{-ik_0x}\right)e^{-i\omega t}$. By measuring the vibrations of three equally-spaced points along the channel ($\eta(x_0,t)$, $\eta(x_0+p,t)$ and $\eta(x_0-p,t)$), we can obtain the complex amplitudes of leftward and rightward waves (A and B) and the wavenumber k_0. Using this method, we can obtain the complex amplitudes of incident (A_i) and transmitted (A_t) waves as well as the transmission ($T = |A_t/A_i|^2$) as shown in the squares in Figs. 2c and 2d.

Calculations based on effective parameters. Consider incidence of a harmonic plane wave on the step as shown in Fig. 1c. The water depth and gravitational acceleration are (g_0, h_0) in the left ($x < 0$) and right ($x > L$) regions and (g_e, h_e) in the middle region ($0 < x < L$). The vertical displacement of water surface can be expressed as: $\eta = \left(A_1e^{ik_0x} + B_1e^{-ik_0x}\right)e^{-i\omega t}$ in the left region, $\eta = \left(A_2e^{ik_ex} + B_2e^{-ik_ex}\right)e^{-i\omega t}$ in the middle region, $\eta = A_4e^{ik_0(x-L)}e^{-i\omega t}$ in the right region. Using the continuities of η and flow $u\nabla\eta$ at the two steps ($x = 0$ and $x = L$), we have $A_1 + B_1 = A_2 + B_2$, $u_0k_0(A_1 - B_1) = u_ek_e(A_2 - B_2)$, $A_3 = A_2e^{ik_eL}$, $B_3 = B_2e^{-ik_eL}$, $A_3 + B_3 = A_4$ and $u_ek_e(A_3 - B_3) = u_0k_0A_4$. Hence, we can obtain the transmission $T = |A_4/A_1|^2$, such as the solid lines in Fig. 2c.

Simulations for real structures. For harmonic water waves in the structures shown in Fig. 1a, the vertical displacement of water surface $\eta e^{-i\omega t}$ satisfies a two-dimensional Helmholtz equation, $\nabla^2\eta + k_0^2\eta = 0$, which is subjected to a no-flow condition $\vec{n}\cdot\nabla\eta = 0$ at the surfaces of vertical walls and split tubes with $\vec{n}$ being the surface normal. The left and right sides of the channel are perfect absorbing boundaries. Hence, we can apply the finite-difference time-domain method or finite-element method to calculate the transmission (dashed lines in Fig. 2c) and mode profiles (Fig. 3).

1. Halliday, D., Resnick, R. & Krane, K. S. *Physics* (John Wiley, New York, 2001).
2. Mei, C. C. *The Applied Dynamics of Ocean Surface Waves* (World Scientific, Singapore, 1989).
3. Heathershaw, A. D. Seabed-wave resonance and sand bar growth. *Nature* **296**, 343–345 (1982).
4. Mei, C. C. Resonant reflection of surface-water waves by periodic sandbars. *J. Fluid Mech.* **152**, 315–335 (1985).
5. Torres, M., Adrados, J. P. & Monterode Espinosa, F. R. Visualization of Bloch waves and domain walls. *Nature* **398**, 114–115 (1999).
6. Hu, X., Shen, Y., Liu, X., Fu, R. & Zi, J. Complete band gaps for liquid surface waves propagating over a periodically drilled bottom. *Phys. Rev. E* **68**, 066308 (2003).
7. Chen, H. Y., Yang, J., Zi, J. & Chan, C. T. Transformation media for linear liquid surface waves. *Europhys. Lett.* **85**, 24004 (2009).
8. Alam, M. R. Broadband Cloaking in Stratified Seas. *Phys. Rev. Lett.* **108**, 084502 (2012).
9. Zhang, Y. *et al.* Band gaps and localization of surface water waves over large-scale sand waves with random fluctuations. *Phys. Rev. E* **85**, 066319 (2012).
10. Chou, T. Band structure of surface flexural-gravity waves along periodic interfaces. *J. Fluid Mech.* **369**, 333–350 (1998).
11. Linton, C. & Evans, D. The interaction of waves with arrays of vertical circular-cylinders. *J. Fluid Mech.* **215**, 549–569 (1990).
12. McIver, P. Water-wave propagation through an infinite array of cylindrical structures. *J. Fluid Mech.* **424**, 101–125 (2000).
13. Hu, X., Shen, Y., Liu, X., Fu, R. & Zi, J. Superlensing effect in liquid surface waves. *Phys. Rev. E* **69**, 030201(R) (2004).
14. Jeong, T. S., Kim, J. E. & Park, H. Y. Experimental measurement of water wave band gaps. *Appl. Phys. Lett.* **85**, 1645 (2004).
15. Farhat, M., Enoch, S., Guenneau, S. & Movchan, A. B. Broadband cylindrical acoustic cloak for linear surface waves in a fluid. *Phys. Rev. Lett.* **101**, 134501 (2008).
16. Yang, J. *et al.* Observation of the focusing of liquid surface waves. *Appl. Phys. Lett.* **95**, 094106 (2009).
17. Griffiths, L. S. & Porter, R. Focusing of surface waves by variable bathymetry. *Applied Ocean Research* **34**, 150–163 (2012).
18. Pendry, J. B., Holden, A. J., Robbins, D. J. & Stewart, W. J. Magnetism from conductors and enhanced nonlinear phenomena. *IEEE Trans. Microwave Theory Tech.* **47**, 2075–2084 (1999).
19. Smith, D. R., Pendry, J. B. & Wiltshire, M. Metamaterials and negative refractive index. *Science* **305**, 788–792 (2004).
20. Smith, D. R. & Pendry, J. B. Homogenization of metamaterials by field averaging. *J. Opt. Soc. Am. B* **23**, 391–403 (2006).
21. Chen, H., Chan, C. T. & Sheng, P. Transformation optics and metamaterials. *Nature Materials* **9**, 387–396 (2010).
22. Soukoulis, C. M. & Wegener, M. Optical metamaterials - more bulky and less lossy. *Science* **330**, 1633–1634 (2010).
23. Xiao, S. *et al.* Loss-free and active optical negative index metamaterial. *Nature* **466**, 735–738 (2010).
24. Choi, M. *et al.* A terahertz metamaterial with unnaturally high refractive index. *Nature* **470**, 369–373 (2011).
25. Liu, Z. *et al.* Locally resonant sonic materials. *Science* **289**, 1734–1736 (2000).
26. Cervera, F. *et al.* Refractive acoustic devices for airborne sound. *Phys. Rev. Lett.* **88**, 023902 (2001).
27. Li, J. & Chan, C. T. Double-negative acoustic metamaterial. *Phys. Rev. E* **70**, 055602 (2004).
28. Hu, X., Chan, C. T. & Zi, J. Two-dimensional sonic crystals with Helmholtz resonators. *Phys. Rev. E* **71**, 055601 (R) (2005).
29. Fang, N. *et al.* Ultrasonic metamaterials with negative modulus. *Nature Mater.* **5**, 452–456 (2006).
30. Lee, S. H., Park, C. M., Seo, Y. M., Wang, Z. G. & Kim, C. K. Composite acoustic medium with simultaneously negative density and modulus. *Phys. Rev. Lett.* **104**, 054301 (2010).
31. Zhu, J. *et al.* F. J. A holey-structured metamaterial for acoustic deep-subwavelength imaging. *Nature Phys.* **7**, 52–55 (2011).
32. Mei, C. C. & Liu, Y.-H. Approximate theory of acoustic waveguides of metamaterials. *J. Fluid Mech.* **678**, 203–220 (2011).
33. Mei, J. *et al.* Dark acoustic metamaterials as super absorbers for low-frequency sound. *Nat. Commun.* **3**, 756, doi: 10.1038/ncomms1758 (2012).
34. Liang, Z. & Li, J. Extreme Acoustic Metamaterial by Coiling Up Space. *Phys. Rev. Lett.* **108**, 114301 (2012).
35. Hu, X. & Chan, C. T. Refraction of water waves by periodic cylinder arrays. *Phys. Rev. Lett.* **95**, 154501 (2005).
36. Hu, X., Chan, C. T., Ho, K. M. & Zi, J. Negative effective gravity in water waves by periodic resonator arrays. *Phys. Rev. Lett.* **106**, 174501 (2011).
37. Budal, K. & Falnes, J. A resonant point absorber of ocean-wave power. *Nature* **256**, 478–479 (1975).
38. Callaway, E. To catch a wave. *Nature* **450**, 156–159 (2007).
39. Cruz, J. *Ocean Wave Energy: Current Status and Future Perspectives* (Springer-Verlag, Berlin, 2008).
40. Engstrom, J., Eriksson, M., Isberg, J. & Leijon, M. Wave energy converter with enhanced amplitude response at frequencies coinciding with Swedish west coast sea states by use of a supplementary submerged body. *J. Appl. Phys.* **106**, 064512 (2009).
41. Garnaud, X. & Mei, C. C. Bragg scattering and wave-power extraction by an array of small buoys. *Proc. R. Soc. A* **466**, 79–106 (2010).
42. Garrett, C. G. B. & McCumber, D. E. Propagation of a Gaussian light pulse through an anomalous dispersion medium. *Phys. Rev. A* **1**, 305 (1970).

Acknowledgements

Author contributions

X.H., J.Z., C.T.C. and K.M.H. initiated the research. X.H. and J.Y. conducted the experiments. X.H. performed analytical derivations and numerical calculations. All the authors discussed the results and contributed to the writing of the paper.

Additional information

Supplementary information accompanies this paper at http://www.nature.com/scientificreports

Competing financial interests: The authors declare no competing financial interests.

How to cite this article: Hu, X.H., Yang, J., Zi, J., Chan, C.T. & Ho, K.M. Experimental Observation of Negative Effective Gravity in Water Waves. *Sci. Rep.* **3**, 1916; DOI:10.1038/srep01916 (2013).